

## ORIGINAL RESEARCH ARTICLE

## Comparative proteomic analysis of hearts from mice with high-fat diet-induced metabolic cardiomyopathy

Zongzhe Jiang<sup>1†</sup>, Mingyang Pang<sup>2†</sup>, and Wei Huang<sup>2,3,4\*</sup><sup>1</sup>Luzhou Key Laboratory of Cardiovascular and Metabolic Diseases, Affiliated Hospital of Southwest Medical University, Luzhou, Sichuan, China<sup>2</sup>Department of Cardiology, Chinese PLA Central War Command General Hospital, Wuhan, 430 010, China<sup>3</sup>Division of Cardiology, Department of Internal Medicine, and Hubei Key Laboratory of Genetics and Molecular Mechanisms of Cardiometabolic Disorders, Tongji Hospital, Tongji Medical College, Huazhong University of Science and Technology, Wuhan, 430 010, China<sup>4</sup>Gene Therapy Center and the Institute of Hypertension, Huazhong University of Science and Technology, Wuhan, 430 010, China**Abstract**

In patients with obesity or type 2 diabetes, the accumulation of lipotoxic by-products in cardiomyocytes leads to apoptosis and contractile dysfunction, eventually resulting in metabolic cardiomyopathy (MC). However, the underlying mechanisms remain unclear. In this study, a comparative proteome analysis was conducted to evaluate the differentially expressed proteins (DEPs) in the hearts of normal mice on standard diet (control group) and of high-fat diet (HFD)-induced MC mice (HFD group). We identified 90 DEPs unique to the control group and 18 DEPs unique to the HFD group. In 90 DEPs unique to the control group, only 74 DEPs were annotated in the gene ontology (GO) database. These annotated DEPs are involved in 114 biological processes, 68 molecular functions, and 174 cellular components. In 18 DEPs unique to the HFD group, only 14 DEPs were annotated in the GO database. These annotated DEPs are involved in 24 biological processes, 22 molecular functions, and six cellular components. Protein levels of two fatty acid metabolism-related enzymes, carnitine palmitoyltransferase 1B (CPT1B) and acetyl-CoA acyltransferase 2 (ACAA2), in the hearts of the mice in control group and HFD group were analyzed by immunostaining and Western blot. The results showed that the protein levels of CPT1B and ACAA2 were elevated in hearts of the mice in HFD group, which were consistent with the proteomic analysis. Our results reveal the differentially expressed proteome related to the progression of MC, providing a series of potential therapeutic targets for MC.

**Keywords:** High-fat diet; Metabolic cardiomyopathy; Proteome analysis

<sup>†</sup>These authors contributed equally to this work.

**\*Corresponding author:**Wei Huang  
(huangwei0521@126.com)

**Citation:** Jiang Z, Pang M, and Huang W, 2022, Comparative proteomic analysis of hearts from mice with high-fat diet-induced metabolic cardiomyopathy. *Global Transl Med*, 1(2): 137.  
<https://doi.org/10.36922/gtm.v1i2.137>

**Received:** June 17, 2022**Accepted:** August 12, 2022**Published Online:** September 15, 2022**Copyright:** © 2022 Author(s).

This is an Open Access article distributed under the terms of the Creative Commons Attribution License, permitting distribution, and reproduction in any medium, provided the original work is properly cited.

**Publisher's Note:** AccScience Publishing remains neutral with regard to jurisdictional claims in published maps and institutional affiliations.

**1. Introduction**

According to the report of The International Diabetes Federation, about 500 million people will become obese and insulin-resistant, while more than 500 million people

will be affected by type 2 diabetes by the year 2040<sup>[1]</sup>. An increasing number of evidence indicates that patients who suffer from glucometabolic perturbations are more susceptible to metabolic cardiomyopathy (MC), which is independent to the presence of hypertension, coronary artery disease, and other comorbidities<sup>[2,3]</sup>. Over 80% of patients who suffered from heart failure are either obese or diabetic<sup>[4,5]</sup>. Notably, the prevalence of MC is expected to rise in the next decades. In patients with glucometabolic perturbations, the accumulation of lipotoxic by-products in cardiac myocyte could lead to myocyte apoptosis and contractile dysfunction, eventually resulting in MC. Detrimental effects on cardiomyocytes in patients with obesity and type 2 diabetes include changes in tissue metabolism, substrate utilization, inflammation, and oxidative stress. These effects are thought to induce heart failure<sup>[6-9]</sup>. However, the underlying mechanisms remain unclear and therapies of MC are yet to be developed.<sup>[2]</sup>

The molecular mechanisms underlying MC are mainly based on metabolic dysregulation, inflammation, fibrosis, oxidative stress, and apoptosis. Although free fatty acids are the preferred energy substrate for cardiac cells, alternative fuel sources, such as glucose, lactate, or ketone bodies, are also utilized by the heart to balance the energy supply and by-products overproduction. In obese or diabetic people, mitochondrial fatty acid  $\beta$ -oxidation is increased due to the hyperglycemia and insulin resistance, which is regulated by the PPAR family-mediated transcriptional machinery. For example, the down-regulation of GLUT4 reduces the uptake of glucose in the cardiac cells<sup>[10]</sup>. Peroxisome proliferator-activated receptor- $\gamma$  coactivator-1  $\alpha$ , estrogen-related receptor  $\alpha$ , NFE2 like BZIP transcription factor 2 (NFE2L2), or nuclear respiratory factor 1 (NRF1) and nuclear factor erythroid 2-related factor 2 (NRF2), which are up-regulated in obesity and diabetes, could promote fatty acid oxidation and shut down glucose oxidation<sup>[11,12]</sup>. It is well known that the increased fatty acid oxidation will lead to lipotoxicity, which subsequently activates the proinflammatory transcription factor such as nuclear factor  $\kappa$ B (NF- $\kappa$ B). NF- $\kappa$ B could increase the downstream targets, such as activator protein 1, nuclear factor of activated T-cells, or NF- $\kappa$ B itself, which carry out numerous autocrine activities, including the secretion of cytokines and chemokines<sup>[13]</sup>. Increased inflammation finally impairs myocardial tissues and causes cardiac remodeling by interstitial fibrosis. In addition, increase fatty acid  $\beta$ -oxidation-induced oxidative stress stimulates the proinflammatory transcription factors and the activation of mitogen-activated protein kinase, involving the proapoptotic c-Jun N-terminal kinase and p38, which promotes cell death in MC<sup>[14]</sup>.

In the present study, we aimed to identify the key differentially expressed proteins (DEPs) and pathways involved in high-fat diet (HFD)-induced MC by analyzing the proteome of hearts from the indicated mice. We compared the DEPs between samples from control and HFD groups. Interestingly, we identified 90 proteins which were only detected in the control group and 18 proteins which were only detected in the HFD group. In these DEPs, most of them belong to the metabolic related process. Our results revealed the differentially expressed proteome related to the progression of MC, which could be a potential therapeutic target for MC.

## 2. Materials and methods

### 2.1. Mice

Eight-week-old male wild-type mice (Chongqing Tengxin Biotechnology Co., Ltd) were fed a standard diet and HFD (60% kcal fat; Research Diets, New Brunswick, NJ, USA), respectively, for 5 months in a specific pathogen-free environment provided by the Experimental Animal Center of Southwest Medical University. The mice were separated into two groups, the control group and the HFD group. The mice were sacrificed to collect the hearts, and all the heart tissue were immediately labeled and stored at  $-80^{\circ}\text{C}$  until protein extraction. Animal protocols were approved by Institutional Animals Ethics Committees of Southwest Medical University (Approval No. 20220225-014).

### 2.2. Preparation of samples for liquid chromatography-tandem mass spectrometry (LC-MS/MS)

To prepare samples for LC-MS/MS, we performed an in-solution digestion by trypsin; the protocol is as follows: (i) 8 M urea was added to 300  $\mu\text{g}$  lysates; (ii) proteins were reduced with 5 mM dithiothreitol and incubated for 45 min at  $56^{\circ}\text{C}$  to reduce disulfide bonds; (iii) mixture was cooled to room temperature and alkylated with iodoacetamide to a final concentration of 20 mM; (iv) the mixture was incubated for 30 min in the dark at room temperature; (v) the mixture was diluted 8-fold with 1 M urea using 10 mM triethylammonium bicarbonate and subsequently digested using 1:20 (w/w) trypsin at  $37^{\circ}\text{C}$  overnight; and (vi) Oasis HLB Cartridge 30 mg (Waters Corporation, Milford, MA, USA) was used to desalt the tryptic digests, and it was lyophilized for the subsequent MS/MS analysis.

### 2.3. Data processing and parameters

LC-MS/MS was used for analysis for the six sets of digested peptides. The dried peptides were re-dissolved in 30  $\mu\text{L}$  0.1% formic acid in UHQ water. The nano-LC-MS experiments were performed using AB Sciex 5600+ mass spectrometer. The sample was applied onto a high-performance liquid

chromatography system (Sciex Co.). The peptides were concentrated on a 1.0-cm precolumn (75- $\mu$ m inner diameter, 360- $\mu$ m outer diameter, C18 5  $\mu$ m, Sciex). The peptides were eluted from the precolumn using a gradient from 100% phase A (0.1% fatty acid aqueous solution) to 45% phase B (0.1% fatty acid, 100% acetonitrile) in 75 min at 300 nL/min directly onto an 15-cm analytical column (75- $\mu$ m inner diameter, 360- $\mu$ m outer diameter, ReproSil-Pur C18 3  $\mu$ m, Sciex). The instrument was operated in a data-dependent mode automatically. Three biological replicates were prepared for each sample using a described parameters (2500V+).

#### 2.4. Data processing and assembly

Raw files from LC-MS were searched using the Mascot search engine human database 3.78 for data processing. Parameters were adjusted for: (i) trypsin digestion, with two maximum missed cleavage points permitted; (ii) length of the digested peptide: 6 – 25; (iii) precursor mass tolerance of 10 ppm and fragment mass tolerance adjusted to 0.2 Da; (iv) dynamic variation oxidation of methionine: static modification carbamidomethyl of cysteine was selected; and (v) false discovery rate: < 1. The level of peptide confidence for the data filter was adjusted to “high.”

#### 2.5. Analysis of DEPs by GO and Kyoto Encyclopedia of Genes and Genomes (KEGG)

Gene ontology (GO) analysis was used to evaluate the biological function of DEPs. Pathways analysis was carried out to further evaluate metabolic or signal transduction pathways using the online PANTHER tools (version 15.0) (<http://pantherdb.org/invalidRequest.jsp>).

#### 2.6. Immunostaining

The myocardial tissues were fixed with 4% paraformaldehyde, and then dehydrated and embedded in paraffin. The hearts were cut into slices with a thickness of 4  $\mu$ m and incubated overnight in a thermostat at 37°C. Then, the slices were put into xylene and alcohol (in a gradient of concentration) for dewaxing. After that, the slices were blocked with 5% bovine serum albumin. After being gently washed with phosphate-buffered saline, the cells were incubated with the primary antibodies, including carnitine palmitoyltransferase 1B (CPT1B) (1:100) and acetyl-CoA acyltransferase 2 (ACAA2) (1:100), overnight at 4°C, and then incubated with secondary antibodies conjugated with cyanine dye 3 (Cy3) for 1 h at room temperature. 4',6-diamidino-2-phenylindole (DAPI) was used for nuclear staining. Finally, the cells were observed under a confocal microscope (Leica, Germany).

#### 2.7. Western blot

Total proteins from cells or tissue were lysed using RIPA buffer, and the protein concentration in the cell lysates was assayed by a protein assay dye reagent concentrate (Bio-Rad, USA). Samples were separated by sodium dodecyl sulfate-polyacrylamide gel electrophoresis (SDS-PAGE) and then transferred to polyvinylidene fluoride (PVDF) membranes (pore size 0.45  $\mu$ m). After being blocked with 5% bovine serum albumin for 1 h, the membranes were incubated with primary antibodies, including CPT1B (1:1000), ACAA2 (1:1000), and tubulin (1:5000) at 4°C overnight. After being washed with TBST, the membranes were incubated with secondary antibodies for 1 h at room temperature. Finally, the protein bands were visualized by enhanced chemiluminescence kit (Santa Cruz, Texas, USA).

### 3. Results

#### 3.1. HFD-induced diabetic cardiomyopathy

Given that over 80% of patients with MC are either obese or diabetic, we employed diet-induced obesity to investigate the differential expressed proteins in the heart tissues between normal heart and mice with MC, which was induced by HFD. The experimental procedure is shown in [Figure 1A](#).

In line with other reports,<sup>[15]</sup> the body weight of the mice in the HFD group almost doubled, and their

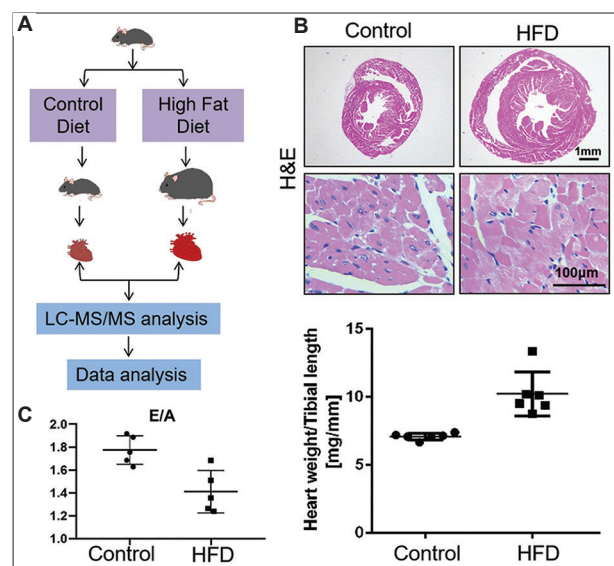


**Figure 1.** High-fat diet (HFD)-induced diabetic cardiomyopathy. (A) Experimental procedure chart for this study. (B) Immunohistochemistry showed an increase of heart volume, cardiac myocyte hypertrophy and an increase of heart weight in HFD-fed mice. (C) Echocardiographic measurement of the diastolic function in standard diet-fed mice or HFD-fed mice.

blood glucose levels also increased after being fed 60% kcal HFD for 5 months. Furthermore, the HFD group with hypertrophic cardiomyocytes had larger and heavier hearts than the control group (Figure 1B). Echocardiographic measurement showed that the diastolic function of hearts from HFD-fed mice were impaired (Figure 1C).

### 3.2. Identification of DEPs

An online tool Venny (Version 2.1) was used to identify DEPs in the hearts of standard diet-fed mice (the control group) and HFD-fed mice (the HFD group). Venn diagrams of data from the control group showed the overlap of identified proteins expressed in Control-1, Control-2, and Control-3. A total of 228 proteins were present in the triplicated control sample (Figure 2A). Venn diagrams of data from the HFD group showed the overlap of identified proteins expressed in HFD-1, HFD-2, and HFD-3. A total of 156 proteins were present in triplicated HFD samples (Figure 2B). A total of 138 common proteins were present in both control and HFD groups in the 3 sets of overlap. A total of 90 proteins were detected in the control group but not in the HFD group. However, 18 proteins were only

detected in the HFD group but not in the control group (Figure 2C).

### 3.3. GO analysis of control group-specific DEPs

To explore the function of DEPs in the heart tissue of wild-type and diabetic mice, we performed GO enrichment analysis for these two groups in the Blast2go (Version 2.5) program and the GO database. As shown in Figure 3, only 74 DEPs were annotated in the GO database among 90 HFD group-specific DEPs. These annotated DEPs are involved in 114 biological processes (Figure 3A), 68 molecular functions (Figure 3B), and 174 cellular components (Figure 3C). In the biological process, 42 DEPs are involved in the clusters of cellular process, and 28 DEPs are involved in the metabolic process (that account for 70/74 in total). The results indicate that HFD reduces proteins associated with the metabolic process in cardiac myocytes.

### 3.4. KEGG analysis of control group-specific DEPs

KEGG is an encyclopedia of genes and genomes that can be used to analyze gene function. It provides a valuable classification for understanding the complex biological functions of genes and genome<sup>[16]</sup>. Therefore, we graphically presented the results of the KEGG annotation analysis to analyze the distribution of DEPs in various pathways. As shown in Figure 4, these annotated DEPs are involved in 51 protein classes (Figure 4A) and 33 pathways (Figure 4B). Furthermore, most DEPs (26 proteins) belong to the cluster of metabolite interconversion enzymes. In the KEGG pathway, the clusters of “cytoskeletal regulation by Rho GTPase,” “glycolysis,” and “gonadotropin-releasing hormone receptor pathway” were the top three pathways that include 3 DEPs, respectively.

### 3.5. GO analysis of HFD group-specific DEPs

As shown in Figure 3, only 14 DEPs are annotated in the GO database in the 18 HFD group-specific DEPs. These annotated DEPs are involved in 24 biological processes (Figure 5A), 22 molecular functions (Figure 5B), and six cellular components (Figure 5C). In the biological process, 20 DEPs are involved in the clusters of cellular processes and 11 DEPs are involved in the metabolic process. The result is consistent with that in control group-specific DEPs, indicating that HFD activates proteins associated with the metabolic process in cardiomyocytes.

### 3.6. KEGG analysis of HFD group-specific DEPs

As shown in Figure 6, these annotated DEPs are involved in nine protein classes (Figure 6A) and seven pathways

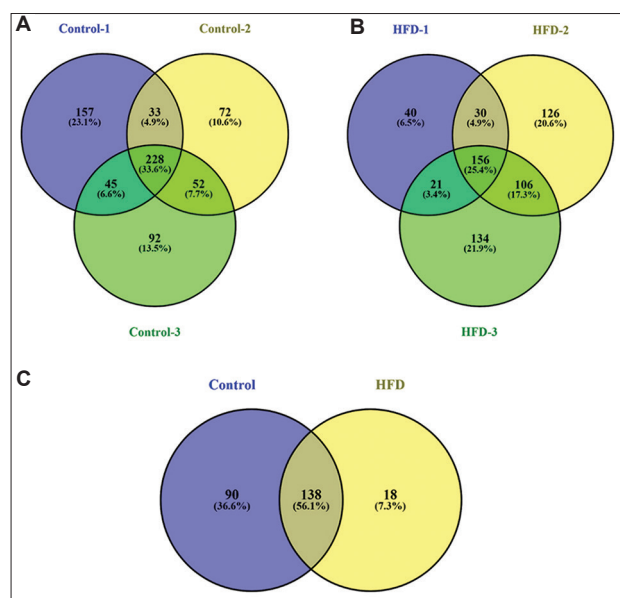


**Figure 2.** Differentially expressed proteins identified in hearts from standard diet-fed mice and high-fat diet (HFD)-fed mice. (A) Venn diagrams show the overlap of identified proteins in triplicate, which were expressed in Control-1, Control-2 and Control-3. A total of 228 proteins were present in triplicated control sample. (B) Venn diagrams show the overlap of identified proteins in triplicate, which were expressed in HFD-1, HFD-2 and HFD-3. A total of 156 proteins were present in triplicated HFD samples. (C) A total of 138 common proteins were present in both control group and HFD groups of the three sets of overlap; 90 proteins were unique to the control group and 18 proteins were unique to the HFD group.

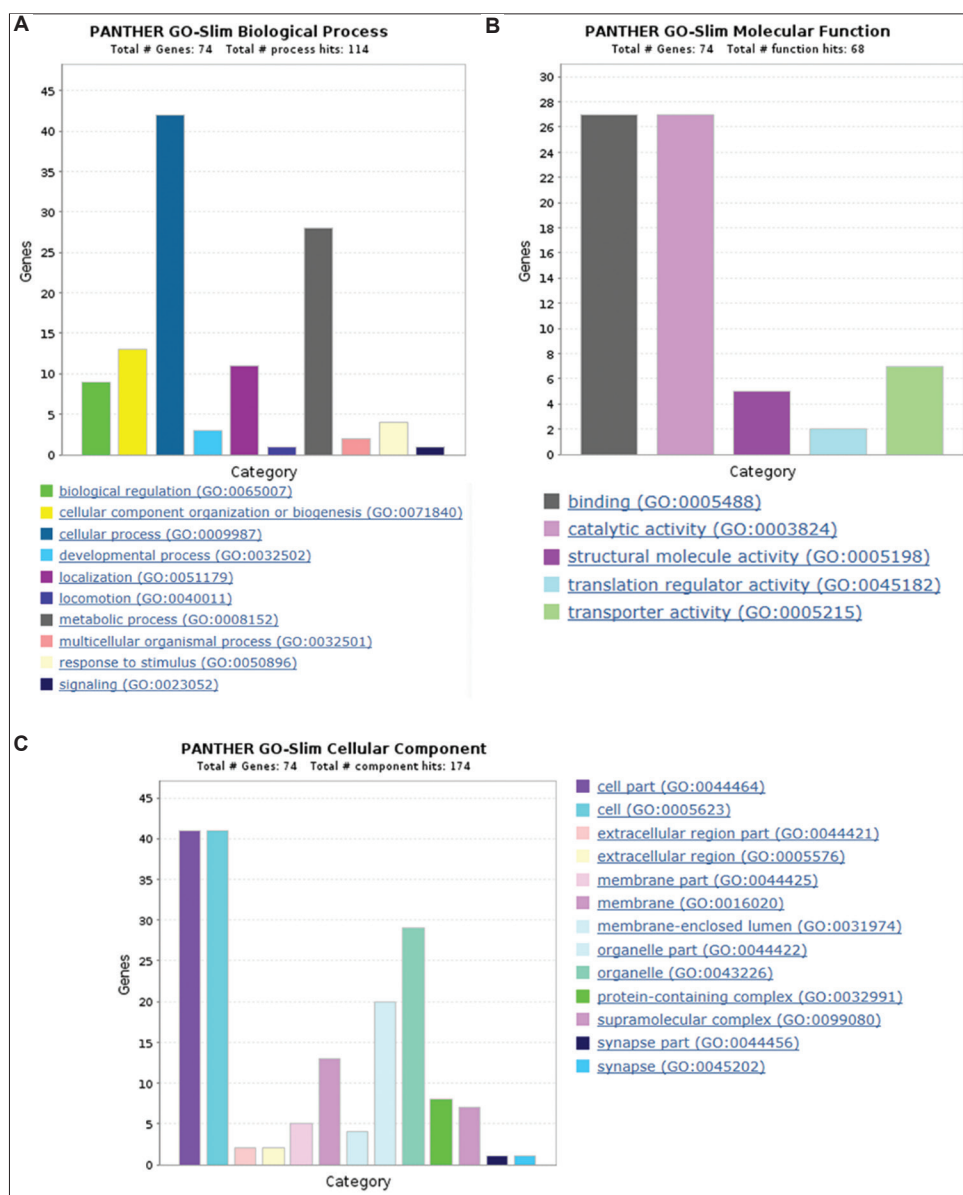


**Figure 3.** Gene ontology analysis of control group-specific differentially expressed proteins. Annotated differentially expressed proteins were distributed in 114 biological processes (A), 68 molecular functions (B), and 174 cellular components (C).

(Figure 6B). Most DEPs are involved in the cluster of metabolite interconversion enzymes (five proteins). The result is consistent with that in control group-specific DEPs. In the KEGG pathway, 7 DEPs were distributed in seven pathways.

### 3.7. Elevation of fatty acid metabolism-related enzymes in the hearts of HFD-fed mice

Since the cluster of metabolite interconversion enzymes has the most DEPs (5 proteins) and fatty acid metabolism plays critical roles in the MC, protein levels of two fatty acid metabolism-related DEPs, CPT1B and ACAA2,

were analyzed by immunostaining and Western blot. The levels of both CPT1B and ACAA2 increased in the hearts of HFD-fed mice (Figures 7 and 8). The result is consistent with the previous proteomic analysis.

## 4. Discussion

Heart failure is the leading cause of MC<sup>[17]</sup>. Many complex molecular mechanisms are reportedly play a role in the pathogenic process of MC. Despite that, the changes of proteome in MC remain unknown. In this study, we used LC-MS/MS to observe the significant difference in proteome between standard diet-fed

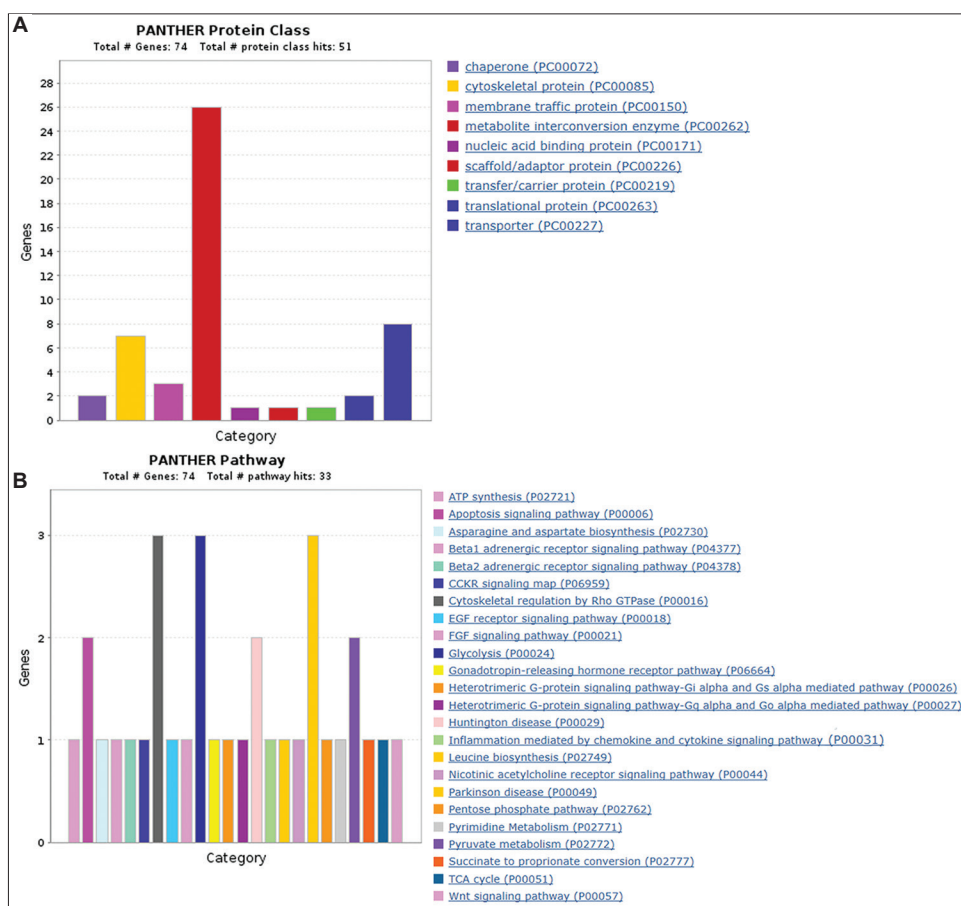


**Figure 4.** Kyoto Encyclopedia of Genes and Genomes analysis of control group-specific differentially expressed proteins. Annotated differentially expressed proteins were distributed in 51 protein classes (A) and 33 pathways (B).

mice and HFD-fed mice. The KEGG analysis of DEGs between standard diet-fed mice and HFD-fed mice showed that, irrespective of control group and HFD group, metabolite interconversion enzyme is the most significant protein. CPT1B and ACAA2 were, further, identified using Western blot and immunostaining. The results demonstrate that the altered expression of metabolite interconversion enzymes is related to MC. As the key enzymes in this pathway, CPT1B and ACAA2 may be potential targets for the treatment of MC.

In the GO enrichment analysis, we found the largest cluster changes in cellular and metabolic processes in both control or HFD group-specific DEPs (Figure 3A and 5A). Among differentially expressed genes (DEGs) involved in cellular and metabolic processes, two succinate dehydrogenase (SDH) family members<sup>[18]</sup>, SDHA and SDHB, led to different expression levels in control and HFD group-specific DEPs. We detected SDHA only in the heart tissue from HFD-fed mice, whereas the SDHB

was observed only in the heart tissue from standard diet-fed mice. The mutation of the *SDHA* gene is related to paraganglioma<sup>[19]</sup>. The *SDHB* mutation can result in pheochromocytoma/paraganglioma syndrome type 4<sup>[20]</sup>. Renal cell carcinoma is a metabolic disease caused by several genes, including *SDH*. The SDH participates in essential cellular processes regulating cell response to sense iron, oxygen, energy, and nutrients<sup>[21]</sup>. Therefore, SDHA and SDHB might play different roles in the progression of MC. We also found that peroxiredoxin V (PRDX5) was absent in the HFD group, in addition to mitochondria-related proteins. PRDX5 is a member of the family of mammalian proteins that neutralize reactive oxygen species<sup>[22]</sup>, which plays a protective role during the early period of small-for-size syndrome in liver transplantation in rats<sup>[23]</sup>. The results suggest that the HFD may lead to the deficiency of protective factors, such as PRDX5, in heart tissue.

The expression data from the KEGG database were analyzed to further identify the differential pathways.

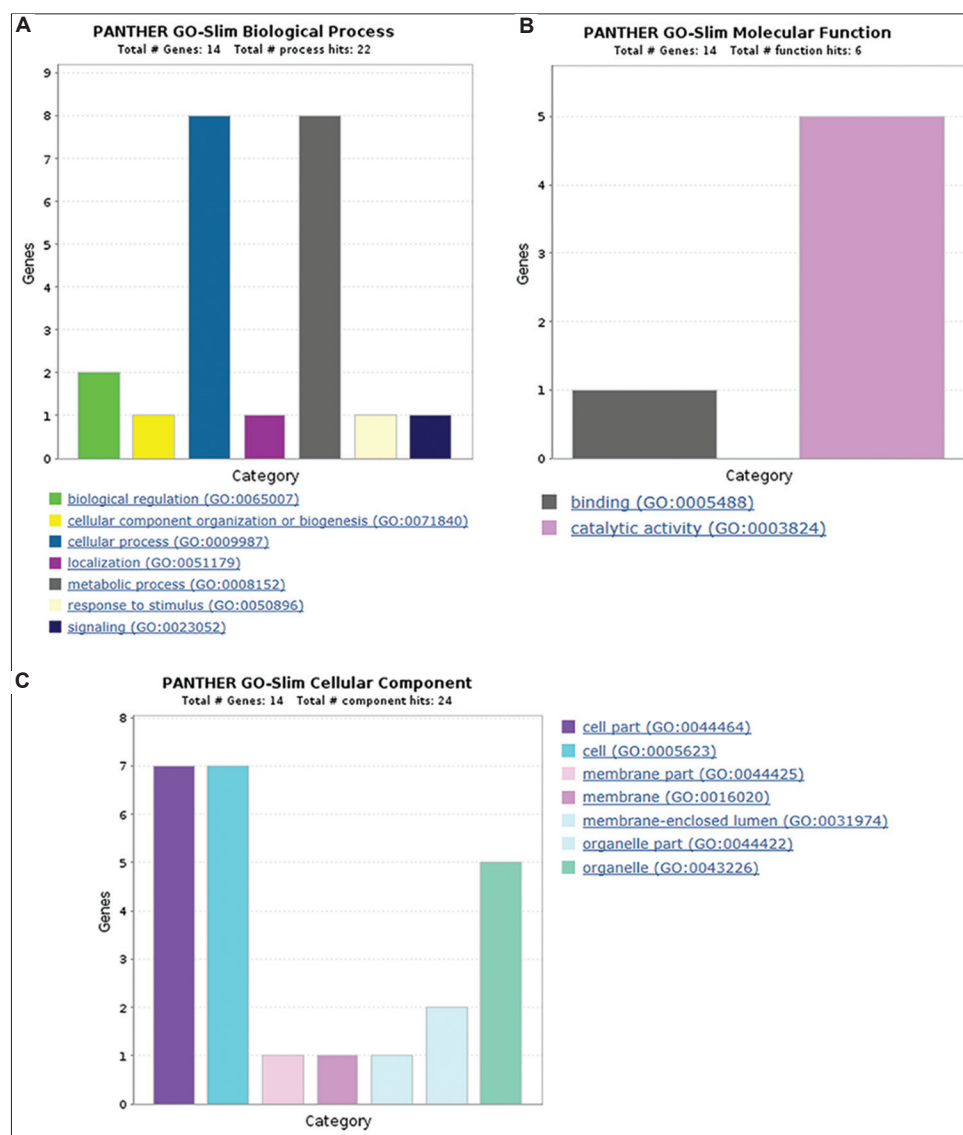


**Figure 5.** Gene ontology analysis of high-fat diet group-specific differentially expressed proteins. Annotated differentially expressed proteins were distributed in 24 biological processes (A), 22 molecular functions (B), and six cellular components (C).

We found that the “metabolite interconversion enzyme” pathway was the most significant in control or HFD group-specific DEPs (Figure 4A and 6A). In addition, two fatty acid metabolism-related DEPs, CPT1B and ACAA2, were only detected in HFD group-specific DEPs by Western blot and immunostaining. CPT1b is a fatty acid metabolism factor that regulates cardiac hypertrophy<sup>[24]</sup>. The deficiency of CPT1B can aggravate cardiac hypertrophy in lipotoxic cardiomyopathy caused by pressure overload<sup>[25]</sup>. In this study, the protein level of CPT1B increased in the hearts of HFD-fed mice,

indicating that the CPT1B adaptively increased under lipotoxicity. ACAA2, an enzyme of the thiolase family, is involved in mitochondrial fatty acid elongation and degradation by catalyzing the last step of the respective  $\beta$ -oxidation pathway<sup>[26]</sup>. Overexpression of ACAA2 and HSD17B12 can inhibit triglyceride production and cell proliferation and induce apoptosis in mammary epithelial cells. In this study, we found that the protein level of ACAA2 increased in the hearts of HFD-fed mice, indicating that the lipotoxicity induced ACAA2 to promote apoptosis.

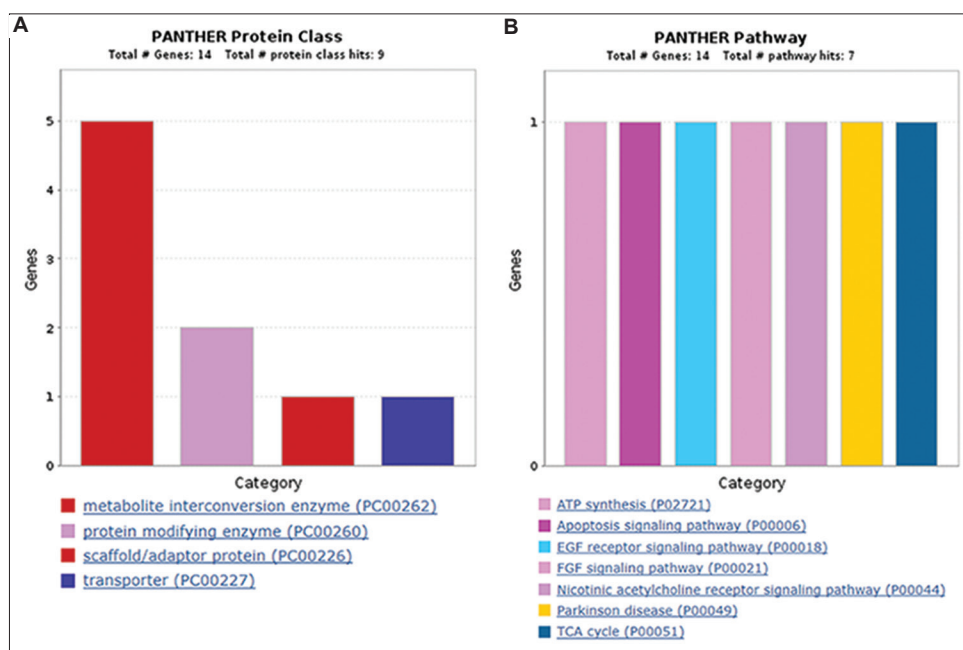


**Figure 6.** Kyoto Encyclopedia of Genes and Genomes analysis of high-fat diet group-specific differentially expressed proteins. Annotated differentially expressed proteins were distributed in nine protein classes (A) and seven pathways (B).

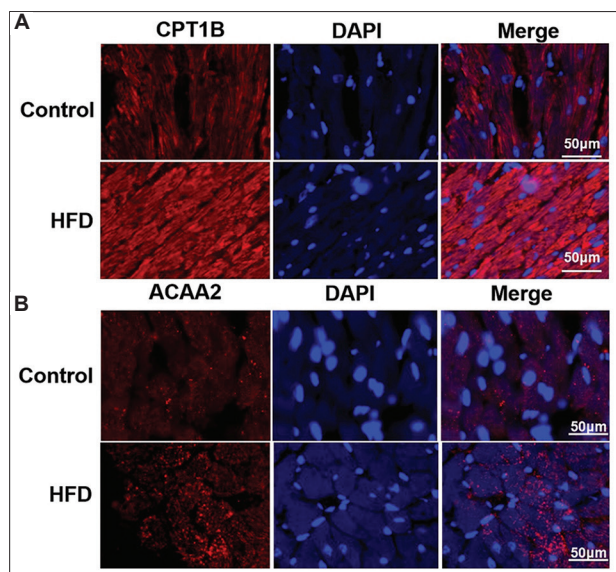


**Figure 7.** Immunostaining of CPT1B and ACAA2. CPT1B (A) and ACAA2 (B) in cardiomyocytes from indicated mice were detected by double labeling immunofluorescence. CPT1B and ACAA2 were labeled by corresponding antibodies (red) and DAPI labeled nucleus (blue).

### 5. Conclusion

Following the comparison of DEPs between samples from the control and HFD groups, we revealed novel DEPs between normal and MC mice. This finding provided essential clues for understanding the specific pathogenetic

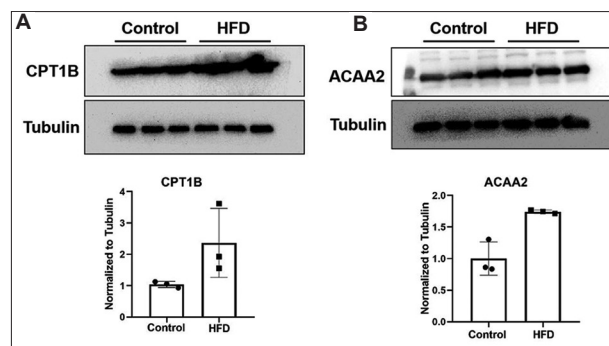


**Figure 8.** Western blot analysis of CPT1B and ACAA2. CPT1B (A) and ACAA2 (B) in cardiomyocytes from indicated mice were detected by Western blot. CPT1B and ACAA2 were incubated with corresponding antibodies and tubulin, which was used as reference. Quantification was performed by imageJ.

mechanisms and potential treatment alternatives for MC. The specific molecular mechanism of metabolic dysfunction in MC needs to be further studied.

### Acknowledgments

We would like to acknowledge Li Rong and Zhang Qi for their supports in data analysis and mass spectrum.

### Funding

This work was supported by grants from the key projects of Sichuan Science and Technology Department (No. 2019YFS0537) and the Doctoral Research Initiation

Fund of Affiliated Hospital of Southwest Medical University (No. 18014).

### Conflict of interest

The authors declare that there are no conflicts of interest regarding the publication of this paper.

### Author contributions

*Conceptualization:* Wei Huang

*Investigation:* Zongzhe Jiang, Mingyang Pang

*Formal analysis:* Wei Huang

*Writing-original draft:* Zongzhe Jiang, Mingyang Pang

*Writing-review and editing:* Huang Wei

### Ethics approval and consent to participate

Animal experiments were approved by the Institutional Animals Ethics Committees of Southwest Medical University (Approval No. 20220225-014). Consent to participate is not applicable.

### Consent for publication

Not applicable.

### Availability of data

The datasets used and analyzed in present study can be obtained from the corresponding author on reasonable request.

### References

- Ogurtsova K, Da Rocha Fernandes JD, Huang Y, *et al.*, 2017, IDF diabetes atlas: global estimates for the prevalence of diabetes for 2015 and 2040. *Diabetes Res. Clin. Pract.*, 128: 40–50.  
<https://doi.org/10.1016/j.diabres.2017.03.024>
- Nishida K, Otsu K, 2017, Inflammation and metabolic cardiomyopathy. *Cardiovasc Res*, 113: 389–398.  
<https://doi.org/10.1093/cvr/cvx012>
- Maack C, Murphy E, 2017, Metabolic cardiomyopathies—fighting the next epidemic. *Cardiovasc Res*, 113: 367–369.  
<https://doi.org/10.1093/cvr/cvx022>
- Obokata M, Reddy YNV, Pislaru SV, *et al.*, 2017, Evidence supporting the existence of a distinct obese phenotype of heart failure with preserved ejection fraction., *Circulation*, 136: 6–19.  
<https://doi.org/10.1161/CIRCULATIONAHA.116.026807>
- Ponikowski P, Voors AA, Anker SD, *et al.*, 2016, 2016 ESC guidelines for the diagnosis and treatment of acute and chronic heart failure: the task force for the diagnosis and treatment of acute and chronic heart failure of the European Society of Cardiology (ESC). Developed with the special contribution of the Heart Failure Association (HFA) of the ESC. *Eur Heart J*, 37: 2129–2200.  
<https://doi.org/10.1093/eurheartj/ehw128>
- Isfort M, Stevens SC, Schaffer S, *et al.*, 2014, Metabolic dysfunction in dia betic cardiomyopathy. *Heart Fail Rev*, 19: 35–48.  
<https://doi.org/10.1007/s10741-013-9377-8>
- Seferovic PM, Paulus WJ, 2015, Clinical diabetic cardiomyopathy: A two-faced disease with restrictive and dilated phenotypes. *Eur Heart J*, 36: 1718–1727, 1727a–1727c.  
<https://doi.org/10.1093/eurheartj/ehv134>
- Authors/Task Force Members, Ryden L, Grant PJ, *et al.*, 2013, ESC guidelines on diabetes, prediabetes, and cardiovascular diseases developed in collaboration with the EASD: the task force on diabetes, pre-diabetes, and cardiovascular diseases of the European Society of Cardiology (ESC) and developed in collaboration with the European association for the study of Diabetes (EASD). *Eur Heart J*, 34: 3035–3087.  
<https://doi.org/10.1093/eurheartj/ehs108>
- Schulze PC, Drosatos K, Goldberg IJ, 2016, Lipid use and misuse by the heart. *Circ Res*, 118: 1736–1751.  
<https://doi.org/10.1161/CIRCRESAHA.116.306842>
- Gibbs EM, Stock JL, McCoid SC, *et al.*, 1995, Glycemic improvement in diabetic db/db mice by overexpression of the human insulinregulatable glucose transporter (GLUT4). *J Clin Invest*, 95: 1512–1218.  
<https://doi.org/10.1172/JCI117823>
- Niture SK, Khatri R, Jaiswal AK, 2014, Regulation of Nrf2-an update. *Free Radic Biol Med*, 66: 36–44.  
<https://doi.org/10.1016/j.freeradbiomed.2013.02.008>
- Tan Y, Ichikawa T, Li J, *et al.*, 2011, Diabetic downregulation of Nrf2 activity via ERK contributes to oxidative stress-induced insulin resistance in cardiac cells *in vitro* and *in vivo*. *Diabetes*, 60: 625–633.  
<https://doi.org/10.2337/db10-1164>
- Jia G, DeMarco VG, Sowers JR, 2016, Insulin resistance and hyperinsulinaemia in diabetic cardiomyopathy. *Nat Rev Endocrinol*, 12: 144–53.  
<https://doi.org/10.1038/nrendo.2015.216>
- Wang Y, Zhou S, Sun W, *et al.*, 2014, Inhibition of JNK by novel curcumin analog C66 prevents diabetic cardiomyopathy with a preservation of cardiac metallothionein expression. *Am J Physiol Endocrinol Metab*, 306: E1239–E1247.  
<https://doi.org/10.1152/ajpendo.00629.2013>
- Winzell MS, Ahren B, 2004, The high-fat diet-fed mouse: A model for studying mecha-nisms and treatment of impaired glucose tolerance and Type 2 diabetes. *Diabetes*, 53: S215–S219.

- [https://doi.org/10.2337/diabetes.53.suppl\\_3.s215](https://doi.org/10.2337/diabetes.53.suppl_3.s215)
16. Kanehisa M, Furumichi M, Tanabe M, *et al.*, 2017, KEGG: New perspectives on genomes, pathways, diseases and drugs. *Nucleic Acids Res*, 45(D1): D353–D61.  
<https://doi.org/10.1093/nar/gkw1092>
17. Costantino S, Akhmedov A, Melina G, *et al.*, 2019, Obesity-induced activation of JunD promotes myocardial lipid accumulation and metabolic cardiomyopathy. *Eur Heart J*, 40: 997–1008.  
<https://doi.org/10.1093/eurheartj/ehy903>
18. Bardella C, Pollard P, Tomlinson I, 2011, SDH mutations in cancer. *Biochim Biophys Acta*, 1807: 1432–1443.  
<https://doi.org/10.1016/j.bbabi.2011.07.003>
19. Burnichon N, Briere JJ, Libe R, *et al.*, 2010, Tssier, Sdha is a tumor suppressor gene causing paraganglioma. *Human Mol Genet*, 19: 3011–3020.  
<https://doi.org/10.1093/hmg/ddq206>
20. Gill AJ, Pachter NS, Chou A, *et al.*, 2011, Tucker, renal tumors associated with germline sdhb mutation show distinctive morphology. *Am J Surg Pathol*, 35: 1578–1585.  
<https://doi.org/10.1097/PAS.0b013e318227e7f4>
21. Ricketts CJ, Shuch B, Vocke CD, *et al.*, 2012, Middleton, succinate dehydrogenase kidney cancer: an aggressive example of the warburg effect in cancer. *J Urol*, 188: 2063–2071.  
<https://doi.org/10.1016/j.juro.2012.08.030>
22. Kropotov A, Usmanova N, Serikov V, *et al.*, 2007, Mitochondrial targeting of human peroxiredoxin V protein and regulation of PRDX5 gene expression by nuclear transcription factors controlling biogenesis of mitochondria. *FEBS J*, 274: 5804–5814.  
<https://doi.org/10.1111/j.1742-4658.2007.06103.x>
23. Wu J, Tang Q, Shen J, *et al.*, 2010, Comparative proteome profile during the early period of small-for-size liver transplantation in rats revealed the protective role of Prdx5. *J Hepatol*, 53: 73–83.  
<https://doi.org/10.1016/j.jhep.2010.01.032>
24. Sun Y, Fan W, Xue R, 2020, Transcribed ultraconserved regions, Uc.323, ameliorates cardiac hypertrophy by regulating the transcription of CPT1b (Carnitine Palmitoyl transferase 1b). *Hypertension*, 75: 79–90.  
<https://doi.org/10.1161/HYPERTENSIONAHA.119.13173>
25. He L, Kim T, Long Q, *et al.*, 2012, Carnitine palmitoyltransferase-1b deficiency aggravates pressure overload-induced cardiac hypertrophy caused by lipotoxicity. *Circulation*, 126: 1705–1716.  
<https://doi.org/10.1161/CIRCULATIONAHA.111.075978>
26. Miltiadou D, Hager-Theodorides AL, Symeou S, *et al.*, 2017, Variants in the 3' untranslated region of the ovine acetyl-coenzyme a acyltransferase 2 gene are associated with dairy traits and exhibit differential allelic expression. *J Dairy Sci*, 100: 6285–6297.  
<https://doi.org/10.3168/jds.2016-12326>